Tet2 deletion in CD4+ T cells disrupts Th1 lineage commitment in memory cells and enhances T follicular helper cell recall responses to viral rechallenge

Andrew Baessler[a] (iD), Bryce Fuchs[a] (iD), Bryant Perkins[a], Andrew W. Richens[a] (iD), Camille L. Novis[a] (iD), Malia Harrison-Chau[a] (iD), Linda M. Sircy[a] (iD), Kendall A. Thiede[a] (iD), and J. Scott Hale[a,1]

Following viral clearance, antigen-specific CD4+ T cells contract and form a pool of distinct Th1 and Tfh memory cells that possess unique epigenetic programs, allowing them to rapidly recall their specific effector functions upon rechallenge. DNA methylation programing mediated by the methylcytosine dioxygenase Tet2 contributes to balancing Th1 and Tfh cell differentiation during acute viral infection; however, the role of Tet2 in CD4+ T cell memory formation and recall is unclear. Using adoptive transfer models of antigen-specific wild type and *Tet2* knockout CD4+ T cells, we find that Tet2 is required for full commitment of CD4+ T cells to the Th1 lineage and that in the absence of Tet2, memory cells preferentially recall a Tfh like phenotype with enhanced expansion upon secondary challenge. These findings demonstrate an important role for Tet2 in enforcing lineage commitment and programing proliferation potential, and highlight the potential of targeting epigenetic programing to enhance adaptive immune responses.

memory T cell | epigenetic | T follicular helper cell | lineage commitment | viral infection

Naïve CD4+ T cells have the capacity to differentiate into one of several effector subsets in response to pathogenic challenge. In the context of viral infection, naïve antigen–specific CD4+ T cells proliferate and differentiate into T helper 1 (Th1) and T follicular helper (Tfh) subsets. Th1 cells express the lineage-defining transcription factor Tbet and migrate to sites of viral infection where they mediate cellular immunity through production of inflammatory cytokines and cytotoxic molecules including IFNγ, TNFα, and Granzyme B (Gzmb) (1, 2). Meanwhile, Tfh cells express Bcl6 and the chemokine receptor CXCR5 and migrate to B cell follicles where they initiate germinal center (GC) formation. Within the GC, Tfh cells provide help to B cells via costimulatory molecules and cytokines including CD40L, IL-21, and IL4 (3–6). These helper signals enable antigen-specific GC B cells to survive, undergo affinity maturation, and differentiate into long-lived plasma cells and memory B cells resulting in a robust antibody response (4–6).

The specialized functions of Th1 and Tfh cells are mediated and maintained by transcriptional and epigenetic programing specific to each cell type. In naïve CD4+ T cells, a limited set of genes necessary for survival and migration are expressed, while genes that contribute to the effector functions of T cells are restricted (7). Epigenetic modifications, including the methylation of cytosine residues within CpG dinucleotides at gene enhancers and promoters, maintain effector genes in a transcriptionally repressed state (8). As naive CD4+ T cells are activated and differentiate into Th1 and Tfh effector subsets, distinct sets of loci are demethylated in each cell type allowing for the expression of lineage-specific genes that enforce commitment and facilitate the unique effector functions of each subset (9). CpG demethylation is mediated by Ten-eleven translocation (Tet) enzymes (8), and Tet2 in particular has been demonstrated to play an important role in the expression of effector genes in Th1, Th17, and regulatory T cells (10–12). In addition, we have shown that during acute viral infection, loss of Tet2 skews the balance of CD4+ T cell differentiation away from Th1 subsets and toward the development of highly functional GC Tfh cells. This skewing was driven in part by failure of *Tet2* knockout (KO) cells to demethylate potent repressors of Tfh differentiation, including Runx2 and Runx3 (13). These findings establish an important role for Tet2 in the differentiation and function of CD4+ T cells.

In addition to regulating T cell differentiation and function, epigenetic modifications also contribute to memory cell development and the ability of memory T cells to rapidly recall effector functions in response to a secondary challenge. Following viral clearance, the majority of activated virus–specific CD4+ T cells are eliminated via apoptosis (7). The remaining cells enter into a memory population that consists of distinct Th1 and Tfh memory subsets that preferentially recall their lineage-specific effector functions upon

Significance

CD4+ memory T cells are critical for providing long-term protection against pathogen reinfection. T follicular helper (Tfh) cells are a subset of CD4+ T cells that provide help for B cells to generate robust antibody responses, and strategies that enhance Tfh memory responses to reinfection could be used to improve vaccination strategies. In this study, we find that in the absence of Tet2, an enzyme that mediates changes in epigenetic programing, CD4+ T cells entering the memory T cell pool after viral clearance are less committed to the T helper 1 cell lineage, and upon reactivation with viral infection, instead recall a robust Tfh cell response that provides enhanced help for B cells.

antigen reencounter (9). Epigenetic programing via CpG demethylation contributes to the recall of specific effector functions, as demethylated effector genes exist in a permissive transcriptional state poised for expression in response to antigen reencounter (9, 14). A recent study reported that Tet2 impacts CD8 T cell memory formation, as loss of Tet2 results in increased CD8+ memory T cells that contribute to enhanced *Listeria monocytogenes* clearance upon a recall response (15). While there is a clear role for DNA methylation and Tet2-mediated programing in T cell memory responses, its role in the formation and recall of memory CD4+ T cells in the context of viral infection remains unknown.

In this study, we examined the role of Tet2 in CD4+ T cell memory formation and recall responses upon secondary viral challenge. Using adoptive transfers of virus-specific wild type (WT) and *Tet2* KO CD4+ T cells, we found that in the absence of Tet2, virus-specific CD4+ T cells do not fully commit to the Th1 lineage. *Tet2* KO Th1 cells generated during acute viral infection have altered methylation programing more similar to that of WT Tfh cells and are able to recall a GC Tfh cell response upon secondary viral challenge. In addition, Tet2-deficient memory CD4+ T cells can expand to a greater extent upon rechallenge and provide enhanced help for B cell responses. These findings demonstrate an important role for Tet2 in modulating the lineage commitment and memory recall potential of CD4+ T cells responding to viral infection and rechallenge.

Results

Tet2-Deficient Memory CD4+ T Cells Possess an Enhanced Ability to Expand in Response to Secondary Challenge. To examine the effects of Tet2 on CD4+ T cell memory differentiation and recall responses, we adoptively cotransferred a 1:1 mix of naïve WT and *Tet2* KO Lymphocytic Choriomeningitis Virus (LCMV) glycoprotein–specific T cell receptor (TCR) transgenic SMARTA (16) CD4+ T cells with distinct congenic markers into recipient C57BL6/J (B6) mice, followed by acute infection with LCMV (*SI Appendix*, Fig. S1 *A and B*). Frequencies of SMARTA cells were monitored longitudinally and 92 d postinfection, WT and *Tet2* KO memory SMARTA cells were harvested from spleens of mice and then cotransferred into new naïve B6 recipient mice, followed by LCMV infection to analyze the memory recall response (*SI Appendix*, Fig. S1A). We found no difference in the frequency of WT vs. *Tet2* KO SMARTA cells in the blood at 7, 15, and 30 days postprimary infection (DPI) (Fig. 1 *A and B*), and no difference in the frequency of WT vs. *Tet2* KO memory cells in the spleen at 92 DPI (Fig. 1C), indicating that loss of Tet2
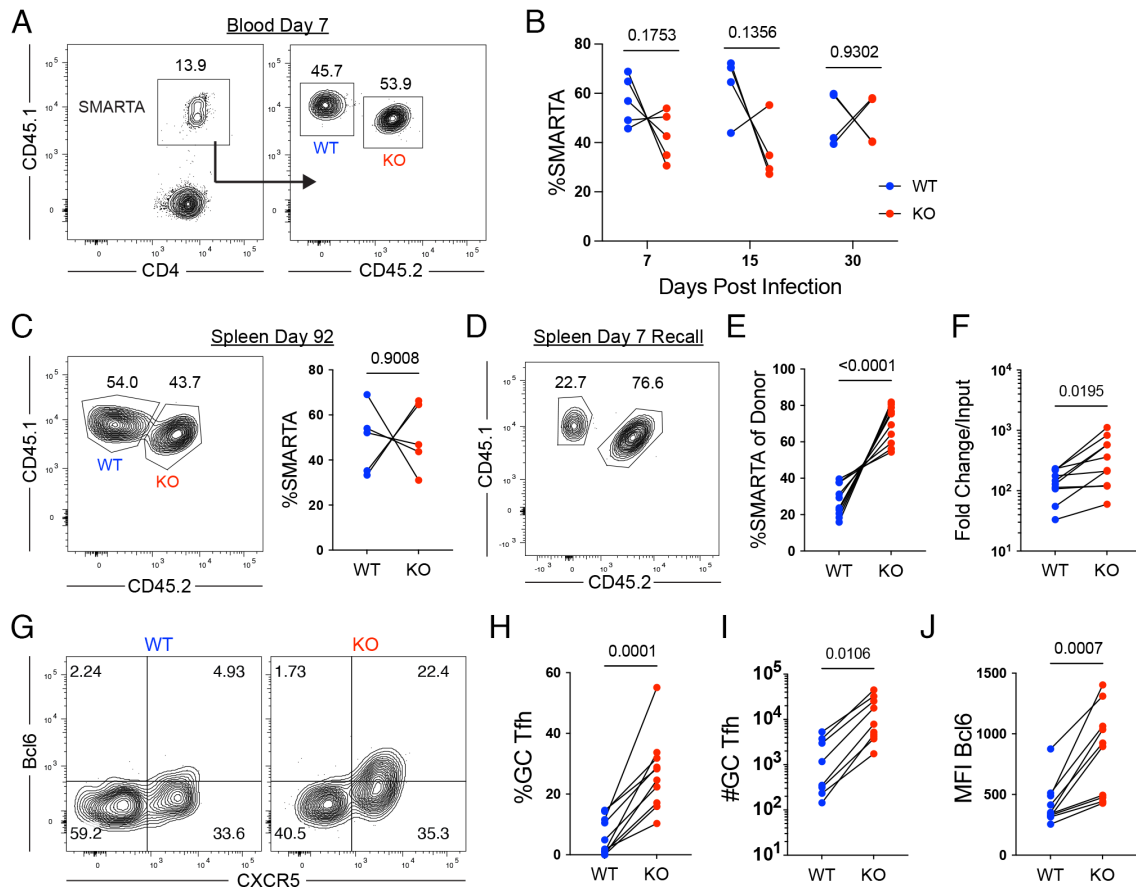

Fig. 1. Tet2-deficient memory CD4+ T cells possess an enhanced ability to expand in response to secondary challenge. (*A and B*) 20,000 congenically marked WT (CD45.1+) and *Tet2* KO (CD45.1+CD45.2+) naïve SMARTA cells were adoptively cotransferred into CD45.2+ naïve B6 recipient mice followed by LCMV Armstrong infection 24 h later and blood was collected at 7, 15, and 30 DPI. (*A*) Gating strategy to identify WT vs. *Tet2* KO cells within the SMARTA population. (*B*) Frequency of WT vs. *Tet2* KO SMARTA cells in the blood at 7, 15, and 30 DPI. (*C–J*) Following transfer and acute LCMV infection, WT and *Tet2* KO memory CD4+ T cells were isolated from spleens at 92 DPI and adoptively transferred into naïve CD45.2+ B6 recipients, and recipient mice were then infected with LCMV Armstrong 24 h later. The memory recall response of transferred cells was analyzed at 7 DPI. (*C*) Representative FACS plots and charts indicate the frequency of SMARTA cells in the spleen at 92 DPI. (*D*) Representative FACS plot of SMARTA cells in the spleen at 7 d postsecondary challenge. (*E*) Frequency of SMARTA cells in the spleen postsecondary challenge. (*F*) WT vs. *Tet2* KO fold change over input. (*G*) Representative CXCR5 and Bcl6 analysis in the spleen. Cells in upper right quadrant are designated as GC Tfh cells. (*H*) Frequency of CXCR5+Bcl6High GC Tfh SMARTA cells. (*I*) Number of CXCR5+Bcl6High GC Tfh SMARTA cells. (*J*) Bcl6 mean fluorescence intensity (MFI) of CXCR5+ SMARTA cells. For (*A–C*) N = 5 WT and n = 5 *Tet2* KO. Data are representative of two independent experiments. For (*D–J*) n = 10 WT and n = 10 *Tet2* KO. Data are pooled from two independent experiments. Significant *P* values of <0.05 are indicated and were determined using a paired Student's *t* test.

does not impact the amount of memory cells generated following resolution of viral infection. However, following transfer and in the subsequent response to a secondary challenge, *Tet2* KO memory cells expanded to a significantly greater extent compared to their WT counterparts (Fig. 1 *D–F*). *Tet2* KO secondary effector cells were found at significantly greater frequencies and numbers than WT cells at multiple anatomic locations including the spleen (*SI Appendix*, Fig. S1 *C and D*), lymph nodes (*SI Appendix*, Fig. S1 *E and F*), and liver (*SI Appendix*, Fig. S1 *G and H*), suggesting that the increase in *Tet2* KO cells was not merely due to increased trafficking from other locations. Tet2-deficient memory cells also preferentially recalled a significantly higher proportion and number of CXCR5^{High}Bcl6^{High} GC Tfh cells (shown in upper right quadrant of FACS plots) with enhanced Bcl6 expression (Fig. 1 *G–J*), mirroring the phenotype we observed among *Tet2* KO effector cells during the primary response to acute viral infection (13). In contrast to *Tet2* KO CD4+ cells generated in response to acute viral infection, which display a slightly diminished capacity to produce cytokines (13), here we found a greater frequency of *Tet2* KO memory cells capable of producing Th1-associated cytokines including IFNγ, IL2, and TNFα (*SI Appendix, Fig. S1 I–K*), as well as a greater frequency of *Tet2* KO triple cytokine producers when compared to their WT counterparts during a recall response (*SI Appendix*, Fig. S1L). Together, these data indicate that while Tet2 deficiency does not impact the number of memory CD4+ T cells generated, the loss of Tet2 enhances the ability of memory CD4+ T cells to expand in response to a secondary challenge. The data also suggest that Tet2-deficient memory cells may have altered restriction of T helper lineage–specific factors during a secondary challenge as *Tet2* KO memory cells were able to give rise to both a greater frequency of GC Tfh cells and a greater frequency of cells producing Th1 associated cytokines.

Tet2-Deficient Memory Tfh Cells Progressively Lose CXCR5 Expression Over Time. To further investigate the impact of Tet2-deficiency on memory cell development, we examined the phenotype of adoptively transferred WT and *Tet2* KO SMARTA cells in the blood at 7, 15, and 30 DPI and in the spleen at 100 DPI (Fig. 2*A*). There was no difference in the frequency of WT vs. *Tet2* KO SMARTA cells in the blood (Fig. 2*B*) and both populations of SMARTA cells declined after 7 DPI, consistent with the expected kinetics of T cell contraction and memory formation (7).

Following primary infection, virus-specific CD4+ T cells form distinct Th1 and Tfh memory subsets (9). Tfh memory cells include CXCR5+Ly6c^{Low} and CXCR5+Ly6c^{Int} subsets, while Th1 memory cells are CXCR5-Ly6c^{High} (9). Consistent with our study of Tet2-deficient CD4+ T cells during primary infection (13), we observed a greater frequency of *Tet2* KO CXCR5+Ly6c^{Low} circulating Tfh cells in the blood at 7 DPI relative to their WT counterparts (Fig. 2 *C and D*). Surprisingly however, the population of *Tet2* KO CXCR5+Ly6c^{Low} cells decreased over time such that there was no difference at day 15, and by day 30 the frequency of *Tet2* KO CXCR5+Ly6c^{Low} cells was significantly lower than WT CXCR5+Ly6c^{Low} cells (Fig. 2 *C and D*). At 100 DPI, while there was no significant difference in the frequency or number of SMARTA cells in the spleen (Fig. 2 *E and F*), there was a significantly lower frequency of *Tet2* KO CXCR5+Ly6c^{Low} cells (Fig. 2 *G and H*) as well as a lower frequency of CXCR5+Ly6c^{Int} cells (Fig. 2*G*). We then examined the population of Ly6c^{Low} SMARTA cells in the spleen at day 100, as the Ly6c^{Low} population contains the majority of memory Tfh cells (9). CXCR5 expression was significantly diminished in Ly6c^{Low} *Tet2* KO cells relative to their WT counterparts (Fig. 2 *I and J*). Together, these data indicate

that *Tet2* KO Tfh memory cells progressively lose CXCR5 expression over time. Interestingly, there was no difference in *Cxcr5* messenger RNA levels comparing WT vs. *Tet2* KO Tfh effector cells 7 DPI (*SI Appendix*, Fig. S2A). In addition, *Tet2* KO memory cells preferentially recall an enhanced GC Tfh phenotype (Fig. 1 *G–J*); therefore, we considered the possibility that continued expression of CXCR5 during the memory phase may depend on Tet2-dependent demethylation. To determine whether Tet2 contributes to demethylation of the *Cxcr5* locus, we analyzed genome-wide methylation data acquired from our study of Tet2-deficient Th1 and Tfh cells 7 d after primary LCMV infection (13). We identified three regions of hypermethylation at the *Cxcr5* locus in *Tet2* KO effector cells compared to WT at 7 DPI (*SI Appendix*, Fig. S2A). Interestingly, two of the hypermethylated regions showed a pattern in which the loci were demethylated specifically in WT Tfh cells (*SI Appendix*, Fig. S2B—first and second regions from the left), suggesting that Tet2-mediated demethylation at these regions could contribute to expression of *Cxcr5* as Tfh cells progress into memory Tfh cells. Together, these results indicate that Tet2-mediated programing contributes to the expression of lineage and memory associated genes. Furthermore, these data suggest that while CXCR5 gene and surface expression are relatively normal in activated day 7 effector *Tet2* KO Tfh cells, Tet2 is required for efficient demethylation of the *Cxcr5* locus and for the maintenance of CXCR5 expression by memory Tfh cells.

We also assessed markers associated with survival, memory differentiation, and T helper lineages expressed by adoptively transferred WT and *Tet2* KO SMARTA cells in the blood at 7, 15, and 30 DPI and in the spleen at 35 DPI. We observed slight increases in the expression of factors that contribute to cellular survival, homeostasis, and memory differentiation, including Bcl2 (only at day 7), CD127, and CD62L among *Tet2* KO cells in the blood (*SI Appendix*, Fig. S3 *A–C*). In addition, at an early memory timepoint (D35), there was a significant increase in the amount of Tet2-deficient central memory cells in the blood and spleen (*SI Appendix*, Fig. S3 *D–F*). Interestingly, the increased central memory cells appeared to derive from the *Tet2* KO memory Th1 (Ly6c^{Hi}CXCR5-) population which was significantly greater in frequency than its WT counterpart (Fig. 2*K*). These results suggest that Tet2-mediated programing may restrain the expression of factors that contribute to CD4+ T cell central memory differentiation. We also examined expression of various lineage-associated transcription factors, chemokine receptors, and survival and proliferation associated genes, most of which showed no difference between WT and Tet2 KO memory cell subsets (*SI Appendix*, Fig. S3 *G–N*), although some differences were seen for PD-1, CD200, CD127, and PSGL1 (*SI Appendix*, Fig. S3 *G–T*). Notably however, *Tet2* KO Th1 early memory cells expressed significantly less Runx2 compared to their WT counterparts (Fig. 2 *L and M*). Runx2 promotes Th1 differentiation and restricts Tfh differentiation (17) and we previously reported that *Runx2* is hypermethylated and significantly underexpressed in *Tet2* KO primary effector CD4 T cells compared to their WT counterparts (13). Thus, Tet2-deficient memory cells retain marks of altered methylation programing that could potentially impact their recall response.

Tet2 Is Required for Full Th Lineage Commitment in Th1 Memory Cells. Given the important role of Runx2 in limiting Tfh differentiation (13, 17) and our observation that early memory CXCR5-Ly6c^{Low} Th1 cells express reduced Runx2 (Fig. 2 *L and M*), we predicted that the reduced expression of Runx2 in Tet2-deficient Th1 memory cells might alter their plasticity to skew the recall response toward a Tfh-like recall response. To determine
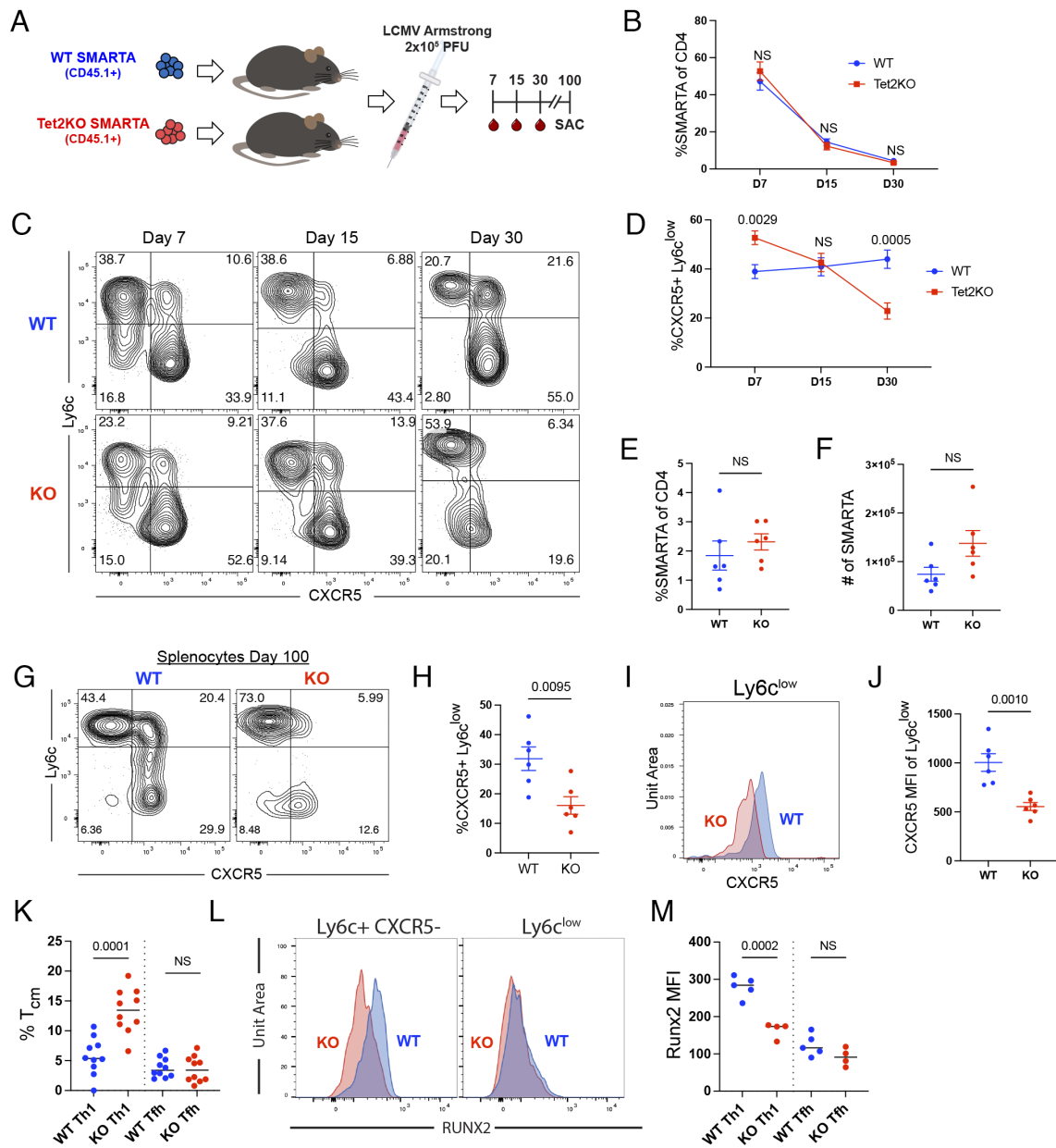
Fig. 2. Tet2-deficient memory CD4+ Tfh cells progressively lose CXCR5 expression over time. (*A–K*) 200,000 congenically marked WT and *Tet2* KO naïve SMARTA CD4+ T cells were adoptively transferred into separate recipient B6 mice followed by infection with LCMV 24 h later. Blood was collected at 7,15, and 30 DPI and SMARTA memory cells in the spleen were analyzed at 100 DPI. (*A*) Experimental setup. (*B*) Frequency of SMARTA cells in the blood at 7, 15, and 30 DPI. (*C*) Representative Ly6c and CXCR5 analysis of SMARTA cells in the blood. (*D*) Frequency of CXCR5+Ly6C^{Low} SMARTA cells in the blood following infection. (*E*) Frequency of SMARTA cells in the spleen at 100 DPI. (*F*) Number of SMARTA cells in the spleen at 100 DPI. (*G*) Representative Ly6c and CXCR5 analysis of memory SMARTA cells in the spleen at 100 DPI. (*H*) Frequency of CXCR5+Ly6c^{Low} memory SMARTA cells in the spleen at 100 DPI. (*I*) Representative CXCR5 histogram of Ly6c^{Low} SMARTA cells in the spleen at 100 DPI. (*J*) CXCR5 MFI of Ly6c^{Low} SMARTA memory cells in the spleen. (*K–M*) 200,000 congenically marked WT and *Tet2* KO naïve SMARTA CD4+ T cells were adoptively transferred into separate recipient B6 mice followed by infection with LCMV 24 h later. SMARTA memory cells in the spleen were analyzed at 35 DPI. (*K*) Frequency of central memory cells (CD62L+) among WT and *Tet2* KO Th1 (Ly6c$^+$ CXCR5$^-$) and Tfh (Ly6c$^-$) cells. (*L*) Representative Runx2 histograms of WT and *Tet2* KO Th1 (Ly6c$^+$ CXCR5$^-$) and Tfh (Ly6c$^-$) cells. (*M*) MFI of Runx2 among WT and *Tet2* KO Th1 (Ly6c$^+$ CXCR5$^-$) and Tfh (Ly6c$^-$) cells. For (*A–J*), n = 6 WT and n = 6 *Tet2* KO. For (*K* and *L*), n = 10 WT and N = 10 Tet KO. For (*M*), n = 5 WT and n = 4 KO. Data are representative of two independent experiments. Gene expression is shown as normalized counts. Statistically significant *P* values of <0.05 are indicated and were determined using an unpaired Student's *t* test.

whether loss of Tet2 impacts lineage commitment of effector Th1 and Tfh cells that persist into the CD4+ T cell memory pool, we used cell sorting to purify *Tet2* KO and WT SMARTA effector cells into Th1 and Tfh populations 7 d after primary LCMV infection (*SI Appendix,* Fig. S4 *A* and *B*). We chose this timepoint because *Tet2* KO cells still express similarly high levels of CXCR5 at day 7 (Fig. 2*C*), and thus Th1 and Tfh cells could be sorted based on CXCR5 and PD1 expression (*SI Appendix,* Fig. S4*B*). The sorted day 7 effector Th1 and Tfh cells were then transferred into separate naïve recipient mice. Sixty days after transfer, mice were

infected with LCMV and the memory recall responses derived from the adoptively transferred effector cells were analyzed in the spleen 7 d postrechallenge (Day 60+7) (*SI Appendix,* Fig. S4*A*). At 7 d post rechallenge there was a significantly greater frequency and number of secondary effector cells from donor *Tet2* KO Th1 SMARTA cells, compared to the other donor populations (Fig. 3 *A* and *B*). This result was consistent with our previous experiment, showing enhanced expansion of *Tet2* KO memory cells upon secondary challenge (Fig. 1 *D–F*) and indicates that the subset of memory cells driving the heightened expansion were
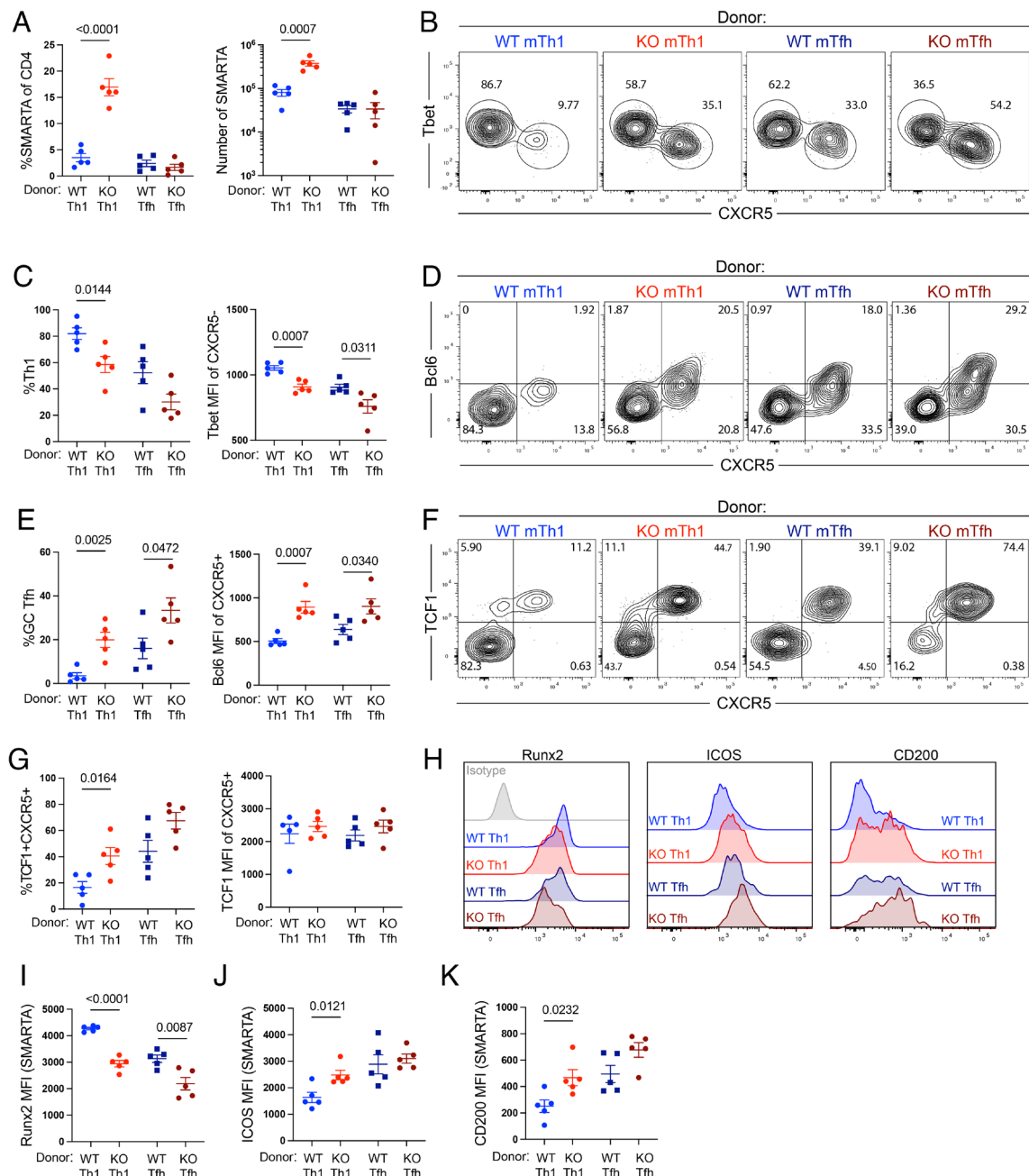
Fig. 3. Tet2 restricts hyperproliferation and Th lineage plasticity of Th1 memory cells. 200,000 congenically marked donor WT and *Tet2* KO naïve SMARTA CD4+ T cells were adoptively transferred into B6 recipients followed by infection with LCMV 24 h later. Donor SMARTA from the spleens of recipient mice at 7 DPI were sorted into CXCR5- Th1 and CXCR5+ Tfh subsets and 200,000 cells from each group were transferred separately into new naïve B6 recipients. Recipient mice were infected with LCMV 60 d posttransfer and 7 d later donor SMARTA cells were analyzed from the spleens. (*A*) Frequency (*Left*) and number (*Right*) of donor SMARTA cells. (*B*) Representative CXCR5 and Tbet analysis of donor SMARTA cells. (*C*) Frequency of Tbet^High^CXCR5- donor SMARTA cells (*Left*) and Tbet MFI of CXCR5- donor SMARTA cells (*Right*). (*D*) Representative CXCR5 and Bcl6 analysis of donor SMARTA cells. Cells in upper right quadrant are designated as GC Tfh cells. (*E*) Frequency of Bcl6^High^CXCR5+ donor SMARTA cells (*Left*) and Bcl6 MFI of CXCR5+ donor SMARTA cells (*Right*). (*F*) Representative CXCR5 and TCF1 analysis of donor SMARTA cells. (*G*) Frequency of TCFf1+CXCR5+ cells (*Left*) and TCF1 MFI of CXCR5+ donor SMARTA cells (*Right*). (*H*) Representative histograms of Runx2, ICOS, and CD200 expression in donor SMARTA cells. (*I–K*) Runx2 (*I*), ICOS (*J*), and CD200 (*K*) MFI in donor SMARTA cells. N = 5 WT and 5 *Tet2* KO. Data are representative of two independent experiments. Significant *P* values of <0.05 are indicated and were determined using an unpaired Student's *t* test.

originally derived from the *Tet2* KO Th1 subset. There were not significant differences among secondary effector cells derived from the donor populations for IFNγ or TNFα expression, although donor *Tet2* KO Tfh cells exhibited enhanced IL2 production compared to donor WT Tfh cells, suggesting that IL2 expression may be inhibited by programing downstream of Tet2-mediated demethylation in Tfh cells (*SI Appendix*, Fig. S4 *C–F*).

Next, we examined the Th lineage recalled during secondary challenge by assessing CXCR5, Bcl6, Tbet, and TCF1 expression.

As expected, memory cells derived from donor WT Th1 cells primarily recalled a Tbet^High^CXCR5- Th1-like phenotype during their secondary response, with limited pluripotency toward the development of CXCR5+ cells (Fig. 3 *B* and *C*) consistent with a previous study (9). In contrast, there were significantly fewer memory cells derived from donor *Tet2* KO Th1 cells that developed into Tbet^High^CXCR5- secondary effector cells upon rechallenge and these cells also expressed less Tbet compared to donor WT Th1 cells (Fig. 3 *B* and *C*). By CXCR5 and Tbet expression,

secondary effector cells from donor *Tet2* KO Th1 cells more closely resembled cells from the donor WT Tfh group, while those from donor *Tet2* KO Tfh cells exhibited the greatest frequency of CXCR5 expression and lowest Tbet expression (Fig. 3 *B* and *C*). We next examined CXCR5 expression paired with Bcl6 and Tcf1, hallmarks of Tfh cells (6). While donor WT Th1 cells exhibited only slight plasticity toward the generation of secondary Bcl6^HighCXCR5+ GC Tfh cells, donor *Tet2* KO Th1 cells developed a substantial population of GC Tfh cells in response to secondary challenge approximately equivalent to that of donor WT Tfh group (Fig. 3 *D* and *E*). Likewise, donor *Tet2* KO Tfh cells generated the largest Bcl6^HighCXCR5+ GC Tfh population upon rechallenge (Fig. 3 *D* and *E*). We also observed a similar result with Tcf1, where donor KO Th1 and KO Tfh populations each developed greater frequencies of Tcf1^HighCXCR5+ cells compared to their WT counterparts (Fig. 3 *F* and *G*). These results suggest that in the absence of Tet2, Th1 cells that enter into the memory pool are not fully committed to the Th1 lineage and can develop into Tfh and GC Tfh cells in response to a secondary challenge.

Tet2 restricts Tfh differentiation during primary viral infection in part by demethylating loci that encode factors that repress Tfh-associated genes (13). These factors include Runx2 and Runx3, transcription factors, which limit Tfh and GC Tfh formation by dampening the expression of key Tfh molecules including Inducible T cell Co-Stimulator (ICOS) and CD200 (17). At day 7 postrechallenge, in secondary effector cells generated from donor *Tet2* KO Th1 and Tfh cells, we found that expression of Runx2 was significantly reduced while expression of ICOS and CD200 were significantly higher (compared to their WT Th1 and Tfh cell counterparts) (Fig. 3 *H–K*). These results suggest that targets of Tet2-mediated demethylation that act to balance Th1 vs. Tfh differentiation during primary viral infection, such as Runx2, also contribute to the proper recall of the Th1 lineage during a secondary challenge and may be important for CD4+ T cells to fully commit to the Th1 lineage.

Tet2-Deficient Secondary Th1 Cells Have a Tfh-Like Epigenetic Program. To examine the underlying epigenetic programs, we identified targets of Tet2-dependent demethylation using whole-genome enzymatic methylation sequencing (WGEMS) on sorted WT and *Tet2* KO secondary Th1 and Tfh cells 7 d after rechallenge. We also compared these data with WGEMS results we previously generated with *Tet2* KO and WT Th1 and Tfh cells during primary viral infection (13). At a global level, the majority of Tet2-dependent differentially methylated regions (DMRs) are shared between Th1 and Tfh cells (*SI Appendix,* Fig. S5*A*), indicating that Tet2 acts to demethylate many of the same targets in both Th1 and Tfh subsets. Analysis of the top 50 DMRs between WT and *Tet2* KO secondary Th1 revealed hypermethylation (in *Tet2* KO) in many genes we had previously identified during primary LCMV infection (13), including genes involved with T cell activation and differentiation such as *Nfatc1, Prdm1,* and *Runx3* (*SI Appendix,* Fig. S5*B*).

To investigate the methylation differences that underlie the enhanced plasticity among Tet2-deficient Th1 cells upon rechallenge, we examined the list of Tet2-dependent DMRs in secondary WT Th1 cells and ranked them according to greatest mean difference compared to secondary WT Tfh cells (Fig. 4*A*). Both primary and secondary WT Th1 cells are demethylated at genes important for Th1 lineage differentiation and effector functions such as *Prdm1, Havcr2, Gzmb,* and *Tbx21,* whereas *Tet2* KO primary and secondary Th1 cells are hypermethylated at these sites and possess a methylation profile that more closely resembles WT Tfh cells at these same loci (Fig. 4*A*). Thus, in the absence of Tet2, Th1 cells remain methylated at genes that promote Th1 differentiation and

functions and skew toward Tfh differentiation during the recall response.

Analysis of Tet2-dependent DMRs in secondary WT Tfh cells ranked according to greatest mean difference between secondary WT Tfh and WT Th1 cells revealed that while primary and secondary WT Tfh cells are demethylated at several regions of the *Cxcr5* locus, both primary and secondary *Tet2* KO Tfh cells remain hypermethylated at these same sites (Fig. 4*B*). Thus, the *Cxcr5* locus remains methylated in secondary Tet2-deficient Tfh cells despite ample CXCR5 surface expression in both primary and secondary Tfh cells (Fig. 3 *B, D,* and *F*). Together, these data suggest that while Tet2-dependent demethylation at the *Cxcr5* locus is not necessary for expression in highly activated Tfh cells during an ongoing antiviral response (whether primary or secondary), it may be necessary to sustain CXCR5 expression Tfh memory cells during homeostasis at the memory phase.

Detailed examination of DMRs at loci of interest including *Prdm1, Cxcr5, Runx2, Runx3, Tbx21,* and *Bcl6* revealed that most DMRs occur in intronic regions, in agreement with previous studies on Tet2-mediated demethylation (18, 19), and showed that the methylation profiles of cells generated during a secondary response are similar to those of the respective cell types during the primary response (Fig. 4 *C* and *D* and *SI Appendix,* Fig. S5 *C–F*). In addition, regions of Tet2-mediated demethylation in the *Cxcr5* locus coincide with intronic regions previously implicated in positive regulation of CXCR5 expression (20). Moreover, key genes encoding transcription factors that promote Th1 differentiation, including *Prdm1, Runx2, Runx3,* and *Tbx21,* were significantly hypermethylated in *Tet2* KO secondary Th1 compared to WT secondary Th1 cells (Fig. 4*C* and *SI Appendix,* Fig. S5 *C–E*). Notably, hypermethylation of *Tbx21* (which encodes Tbet) and *Runx2* correspond with reduced expression of Tbet and Runx2 during the recall response (Fig. 3 *B, C, H,* and *I*). Together, these data suggest that Th1 recall responses during secondary challenge are reinforced by Tet2-mediated demethylation of key Th1 transcription factors including Tbx21 and Runx2. In the absence of Tet2-mediated programing, Th1 cells acquire a methylation profile resembling that of Tfh cells and consequently skew toward Tfh differentiation upon rechallenge.

Tet2-Deficient Memory CD4+ T Cells Provide Enhanced Help for B Cells in Response to a Secondary Challenge. Given the significant expansion of *Tet2* KO memory cells following rechallenge (Fig. 1 *D–F*), as well as the enhanced GC Tfh phenotype displayed by the *Tet2* KO CD4+ memory T cells during secondary infection (Figs. 1 *G–J* and 3 *D* and *E*), we hypothesized that *Tet2* KO memory CD4+ T cells would be capable of providing enhanced help to B cells in response to a secondary infection. To test this hypothesis, we transferred either WT or *Tet2* KO SMARTA memory cells (generated from adoptive transfer and LCMV infection) into Tfh cell-deficient Bcl6^flox/floxxCD4cre recipient mice, followed by infection with LCMV Armstrong (Fig. 5*A*). Bcl6^flox/floxxCD4cre mice lack endogenous Tfh cells, thus only donor CD4+ T cells can provide help for the B cell response (21, 22). We also included no transfer (NT) Bcl6^flox/floxxCD4cre mice as a control, which were likewise infected with LCMV (Fig. 5*A*). We observed a significant increase in both the frequency and number of secondary effector *Tet2* KO SMARTA cells when compared to WT transfer at 10 d post rechallenge (Fig. 5*B*). As expected, mice in the control NT group had no endogenous CXCR5+ Tfh cells, whereas both WT and *Tet2* KO recipients possessed a clear population of CXCR5+ Tfh SMARTA cells (Fig. 5*C*). In addition, there was a trending increase in the frequency and a significant increase in the number of *Tet2* KO secondary effector GC Tfh cells compared to WT GC
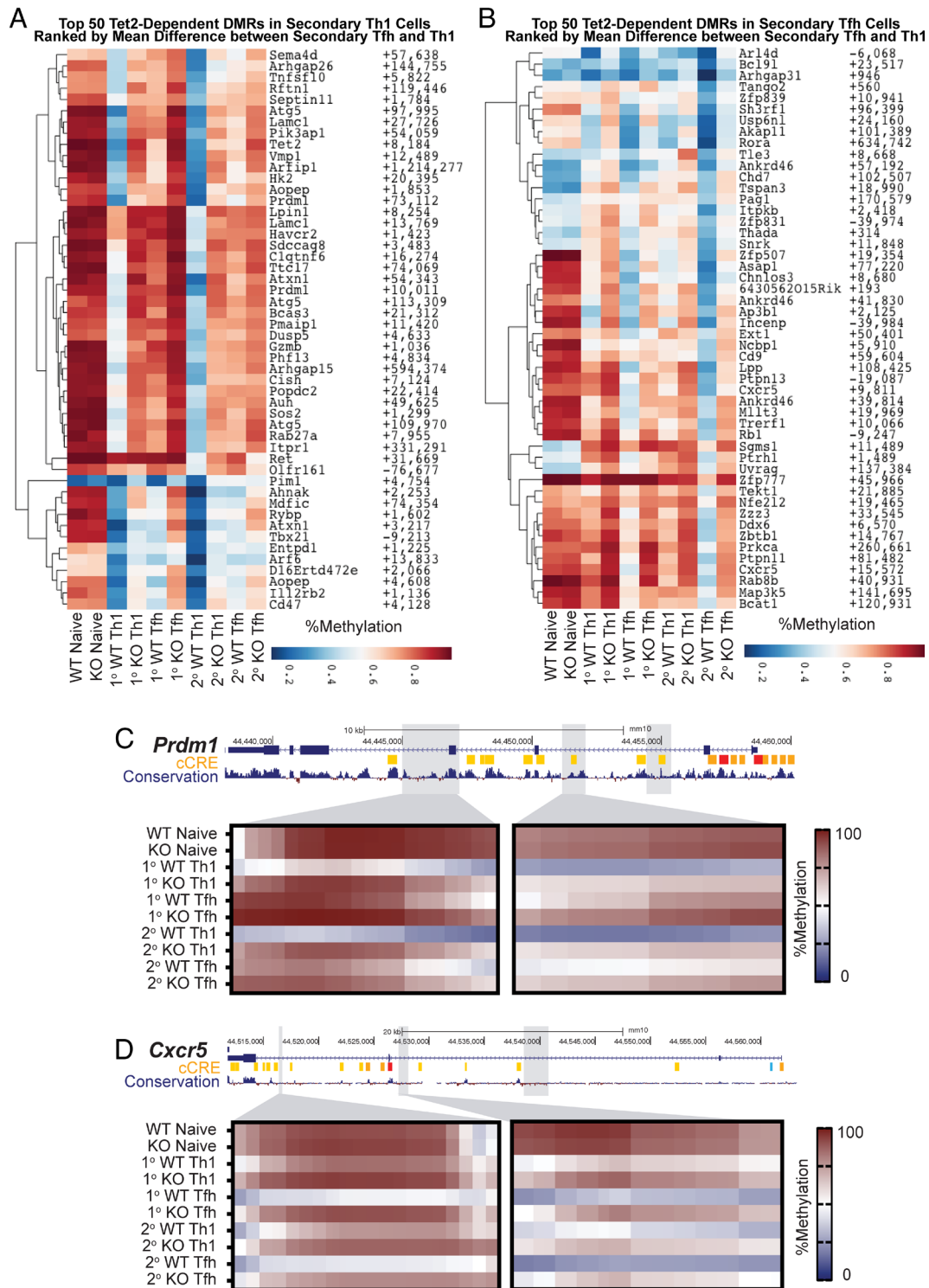
Fig. 4. Tet2 mediates lineage specific demethylation programing in secondary Tfh and Th1 cells. Genome-wide methylation analysis was performed using DNA isolated from WT and *Tet2* KO secondary (2°) effector Th1 and 2° Tfh cells sorted from recipient mice at 7 d post LCMV infection. Statistically significant DMRs were identified between WT and *Tet2* KO Th1 cells as well as WT and Tet2 KO Tfh cells. DMRs were then ranked by the mean difference between secondary WT Tfh and secondary WT Th1 cells. (*A*) Heatmap of the top 50 Tet2-dependent DMRs in secondary Th1 cells ranked by largest mean difference to secondary WT Tfh cells. (*B*) Heatmap of the top 50 Tet2-dependent DMRs in secondary Tfh cells ranked by largest mean difference to secondary WT Th1 cells. (*C* and *D*) UCSC Genome Browser plots of (*C*) Prdm1 and (*D*) Cxcr5 with candidate cis-regulatory regions (cCREs) and mammalian conservation tracks. DMRs are marked with gray shading. Accompanying heatmaps depict the methylation of individual CpG sites within the selected DMRs. For (*A–D*), sample numbers were: WT naïve (n = 3), KO naïve (n = 3), primary (1°) WT Th1 (n = 3), 1° WT Tfh (n = 3), 1° KO Th1 (n = 3), 1° KO Tfh (n = 3), 2° WT Th1 (n = 3), 2° WT Tfh (n = 3), 2° KO Th1 (n =2) and 2° KO Tfh (n = 2). Heatmaps depict the average methylation across the samples in each group and are also representative of individual samples.

Tfh cells (Fig. 5*D*). In agreement with our hypothesis, we observed a significant increase in both the frequencies and numbers of Fas+PNA+ GC B cells and IgD-CD138+ plasmablasts in spleens of mice that received *Tet2* KO memory cells compared to mice

that received WT memory cells (Fig. 5 *E–H*). Collectively, these results demonstrate that *Tet2* KO memory cells are capable of providing significantly enhanced help to support GC B cells during a secondary viral challenge.
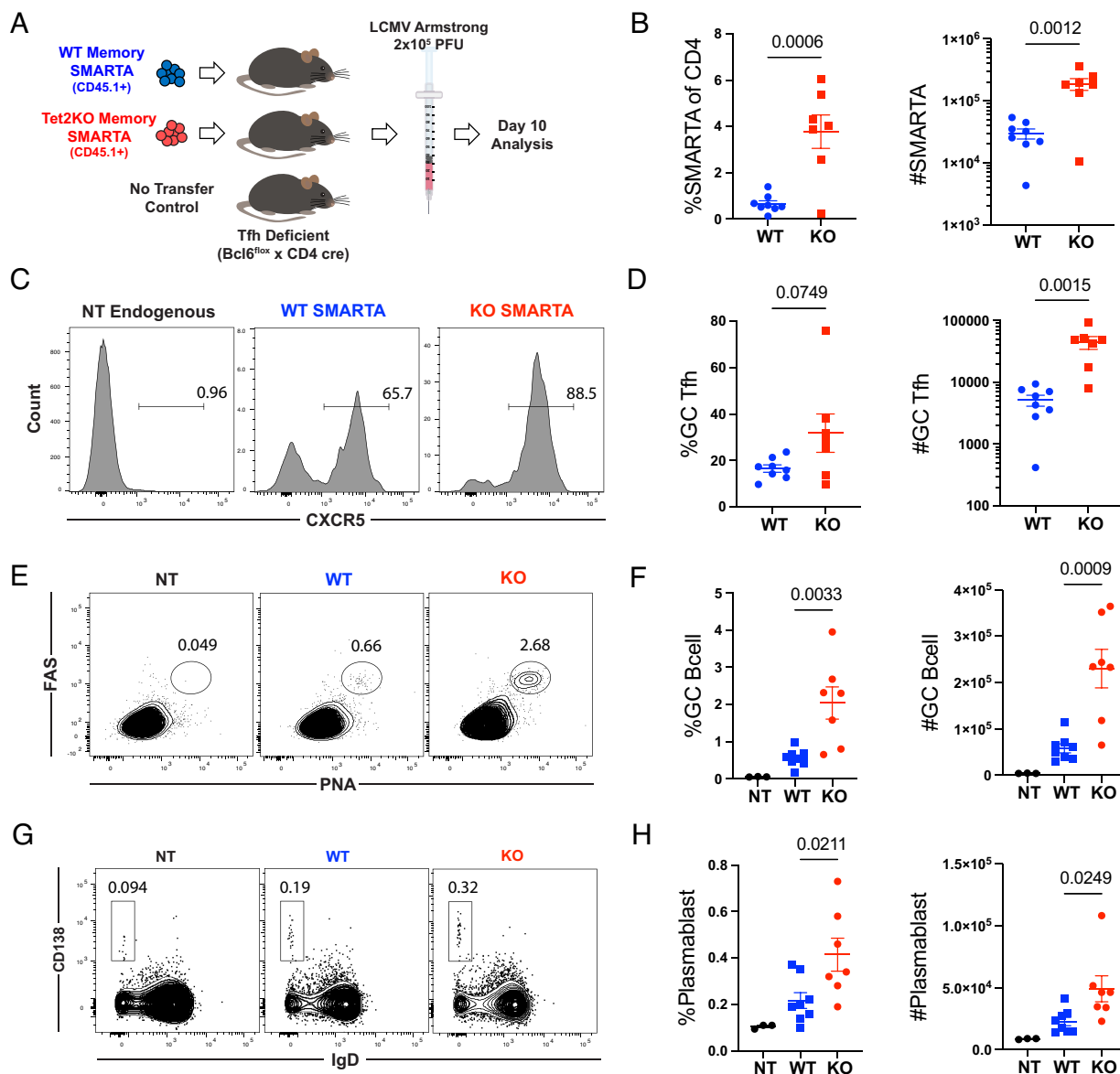
Fig. 5. Tet2 deficient memory CD4+ T cells provide enhanced help for B cells during a secondary challenge. Memory WT and *Tet2* KO SMARTA CD4+ T cells were isolated from the spleens of adoptive recipient mice 57 d after primary LCMV infection. Then, 1,000 isolated WT and *Tet2* KO SMARTA memory cells were transferred into separate congenically marked Bcl6^flox/flox^xCD4cre (Tfh cell-deficient) recipient mice followed by infection with LCMV and analysis of T cell and B cell responses in the spleen at 10 d postrechallenge. (*A*) Experimental setup. (*B*) Frequency and number of SMARTA cells. (*C*) Representative histograms of CXCR5 staining on endogenous CD4+ T cells in the NT group and on WT and *Tet2* KO SMARTA CD4+ T cells in the adoptive transfer recipient groups. (*D*) Frequency and number of GC Tfh cells. (*E*) Representative FACS plots of CD19+ GC B cells (Fas+PNA+) in the spleen. (*F*) Frequency and number of GC B cells. (*G*) Representative FACS plots of CD19+ plasmablasts (IgD-CD138+) in the spleen. (*H*) Frequency and number of plasmablasts. N = 8 WT and n = 7 *Tet2* KO. Data shown are from one experiment and are representative of two independent experiments. Statistically significant *P* values of <0.05 are indicated and were determined using an unpaired Student's *t* test.

Discussion

Tet2-mediated demethylation at gene enhancers and promoters is a major component of epigenetic programing that contributes to cellular differentiation and lineage-specific effector functions of CD4+ T cells (10–13). Changes to DNA methylation status can be propagated to daughter cells and act as an inherited program allowing memory T cells to quickly recall their unique gene expression profiles and effector functions during a secondary challenge (9, 14). While the role of Tet2-mediated demethylation was recently investigated in the context of CD8 T cell memory development (15), its role in CD4+ T cell memory formation remains unclear. In this study, using adoptive transfer of virus-specific memory CD4+ T cells, we show that loss of Tet2 enhances the expansion of memory CD4+ T cells upon secondary viral challenge and that Tet2-deficient memory cells preferentially recall a GC Tfh phenotype with the capacity to provide enhanced help for GC B cell responses. The dramatically increased expansion during the secondary response was primarily driven by *Tet2* KO memory cells derived from the Th1 effector cells that had reduced Th1-lineage commitment and thus possess the capacity to recall a Tfh-like cell response upon secondary infection. Our findings indicate that Tet2-mediated programing limits the secondary expansion by memory CD4+ T cells and is necessary for the full commitment of CD4+ T cells to the Th1 lineage; thus, loss of Tet2 surprisingly results in a block of Th1-lineage commitment, resulting in plastic cells that can generate robust GC Tfh secondary responses.

In CD8+ T cells, loss of Tet2 contributes to enhanced CD8 central memory cell differentiation and Tet2-deficient memory CD8 T cells are capable of providing enhanced protection against a secondary *Listeria monocytogenes* challenge (15). In our study of virus-specific CD4+ T cells, we found that Tet2-deficient CD4+ T cells in the blood displayed enhanced expression of memory and survival associated molecules including CD62L and CD127. However, despite enhanced expression of these molecules, loss of Tet2 did not result in increased numbers of antigen-specific memory CD4+ T cells. Instead, we found that *Tet2* KO memory cells displayed significantly enhanced expansion in response to a secondary viral challenge, accumulating to greater numbers in the spleen compared to their WT memory counterparts. The enhanced expansion only occurred in the context of rechallenge, as we have previously reported that there is no difference in the frequency or number of *Tet2* KO vs. WT SMARTA cells 7 d after primary LCMV infection (13). These results suggest that Tet2-mediated demethylation contributes to the expression of genes that limit cellular proliferation for memory T cell recall responses.

We were initially surprised to find a significant decrease in the population of *Tet2* KO CXCR5+Ly6c^{Low} cells; however, this did not represent a loss of Tfh memory cells, but instead, a loss of CXCR5 expression by memory Tfh cells. We propose that Tet2-mediated demethylation is not necessary for CXCR5 expression in activated primary or secondary effector cells during active antiviral responses, but is needed to enable the maintenance of CXCR5 expression by resting memory CD4+ T cells following viral clearance. Therefore, unlike WT memory Tfh cells, *Tet2* KO memory Tfh cells cannot be distinguished by CXCR5 expression and are partially "hidden" within CXCR5-negative populations in the blood and spleen. In support of this conclusion, we identified DMRs within the *Cxcr5* locus that were significantly hypermethylated in Th1 and Tfh *Tet2* KO SMARTA cells compared to WT Th1 and Tfh SMARTA cells 7 d after primary LCMV infection. Moreover, these regions remained hypermethylated in Tet2-deficient secondary effector cells 7 d after LCMV rechallenge despite reexpression of CXCR5 in Tfh cells in response to rechallenge. Thus, repressive hypermethylation at the *Cxcr5* locus can be overcome during an active anti-viral response, but in resting memory cells, hypermethylation impairs CXCR5 expression.

By sorting and transferring effector WT and *Tet2* KO Th1 and Tfh cells into separate recipient mice at 7 d postprimary infection and then waiting for memory T cell differentiation to occur, we were able to evaluate the distinct impact of Tet2 deficiency on the recall response of Th1 vs. Tfh memory CD4+ T cell populations. We observed a significantly higher frequency and number of secondary effector cells derived from donor *Tet2* KO Th1 cells present in the spleen at 7 days postsecondary challenge when compared to all other donor populations, indicating that Tet2-deficient Th1-derived memory cells were responsible for the significantly enhanced expansion of *Tet2* KO memory CD4+ T cells. The reason behind the specific expansion of *Tet2* KO Th1-derived memory cells is not immediately clear; however, this specific subset acquired a higher frequency of Tcm cells which are associated with greater proliferative potential (7). This occurrence may stem from a failure of Tet2-deficient Th1 cells to fully commit to the Th1 lineage and undergo terminal differentiation. In CD8 T cells, the transcription factor Blimp1 (encoded by *Prdm1*) contributes to terminal differentiation, while its antagonist Bcl6 promotes CD8 T cell memory differentiation (23). Several studies have also shown that Bcl6-mediated repression of Blimp1 contributes to CD4+ T cell memory differentiation (24, 25). Interestingly, we previously identified several sites of hypermethylation within the *Prdm1* locus of *Tet2* KO Th1 cells compared WT Th1 cells, suggesting that

Tet2 may contribute to Blimp1 expression in Th1 cells (13). Thus, in the absence of Tet2, reduced Blimp1 expression could allow Th1-like memory cells to adopt a less Th1-committed and more plastic phenotype that allows for differentiation into Tfh cells during the recall response. We previously reported that key repressors of Tfh differentiation, including Runx2 and Runx3, remain hypermethylated and exhibit reduced expression in Tet2 *KO* cells during primary viral infection, while targets of Runx2/3-mediated repression, such as ICOS and CD200, were more highly expressed (13). Interestingly, in this present study, we also observed reduced expression of Runx2 in both memory cells as well as secondary effector cells derived from *Tet2* KO donor Th1 and Tfh cells during secondary challenge, and a corresponding increase in expression of ICOS and CD200. Therefore, we propose that in Tet2 KO cells, reduced Blimp1, Runx2, and Runx3 decreases Th1-lineage commitment during primary infection that enables subsequent Th1-effector-derived memory cells to become GC Tfh cells during a recall response. Furthermore, analysis of genome-wide methylation profiles during secondary challenge indicates that despite their Th1 effector phenotype at day 7 (13), *Tet2* KO Th1 cells have a DNA methylation epigenomic profile that is more similar to that of WT Tfh effector cells. Collectively, these results demonstrate that Tet2-mediated demethylation is necessary for the full commitment of primary Th1 effector cells to the Th1 lineage, and in the absence of such programing virus-specific Th1 cells form a memory population with enhanced proliferation potential and Th lineage pluripotency during a secondary challenge. Curiously, while methylation and gene expression changes indicate that Tet2-deficient Th1 cells skew toward the Tfh lineage upon rechallenge, these cells were still capable of producing IFNγ. Given their Tfh-like methylation programing, it is not entirely clear why *Tet2* KO cells are capable of IFNγ production, however, the altered programming of many genes and pathways in the absence of Tet2 may contribute to IFNγ expression.

Tfh cells play a critical role in the adaptive immune system and are necessary to generate effective long-lasting antibody responses. Therefore, strategies that enhance the number and/or quality of GC Tfh cells may be useful in the development of new vaccines against pathogens for which current immunizations are not effective (6, 26–30). In this study, we found that Tet2-deficient memory CD4+ T cells provided enhanced help for B cells upon secondary viral challenge, resulting in increased numbers of GC B cells and plasmablasts. This result highlights the potential for targeting epigenetic programing to improve humoral immunity. Furthermore, our study identified a role for Tet2-mediated programing in enforcing commitment of CD4+ T cells to the Th1 lineage. In the absence of such programing, memory Th1 cells were capable of adopting a GC Tfh phenotype upon rechallenge. Given these results, it may be possible to target Tet2 or downstream Tet2-mediated programing at the memory and recall stage to shift Th1 memory cells toward a Tfh lineage and improve immunization responses. Future studies will be needed to determine the precise timing wherein Tet2 contributes to the full lineage commitment of Th1 cells and whether Tet2 could be targeted therapeutically to enhance immunization responses.

Materials and Methods

Mice and Adoptive Transfers. C57BL/6 mice were purchased from The Jackson Laboratory. *Tet2* KO mice (31) were crossed to SMARTA TCR transgenic mice (16) to generate *Tet2* KO×SMARTA mice. For adoptive transfer experiments, congenically marked naïve CD4+ T cells were isolated from the spleens of WT SMARTA (CD45.1$^+$) and *Tet2* KO SMARTA mice (CD45.1$^+$ CD45.2$^+$), combined at a 1:1 ratio, and intravenously cotransferred into naïve C57BL/6 mice (CD45.2), or were transferred into separate mice. Approximately 24 to 72 h after transfer, recipients

were infected intraperitoneally with LCMV Armstrong. For B cell help experiments, congenically marked CD45.1[+] WT or *Tet2* KO naïve SMARTA memory cells were adoptively transferred into CD45.2[+] *Bcl6^flox* × *CD4cre* (T$_{FH}$ cell–deficient) recipient mice (21) followed by infection with LCMV Armstrong approximately 24 h later. All donor mice were between 6 and 8 wk of age. Animal experiments were conducted in accordance with University of Utah Institutional Animal Care and Use Committee–approved protocols.

FACS Analysis and Sorting. Cells were stained in 1× phosphate-buffered saline supplemented with 2% fetal bovine serum (FBS) for 30 min on ice with fluorochrome-conjugated antibodies (purchased from Becton Dickinson (BD) Biosciences, eBioscience, BioLegend, and Invitrogen) for cell surface antigens. The Runx2 antibody was purchased from Cell Signaling Technology (98059s). For CXCR5 staining, a three-step protocol was followed as described in ref. 32 using purified rat anti-mouse CXCR5 (BD Biosciences), a secondary Biotin-SP–conjugated AffiniPure F(ab')$_2$ goat anti-rat immunoglobulin G (IgG) (Jackson ImmunoResearch), and a streptavidin-APC or streptavidin–phycoerythrin–cyanine 7 (Invitrogen). To label transcription factors, cells were first stained for surface antigens followed by permeabilization, fixation, and staining using the Foxp3 Permeabilization/Fixation kit and protocol (eBioscience). For intracellular cytokine staining, cells were first stimulated with GP$_{61–80}$ peptide and brefeldin A (GolgiPlug, BD Biosciences) for 5 h. Cells were then stained for surface antigens followed by permeabilization, fixation, and staining using the Cytofix/Cytoperm kit and protocol (BD Biosciences). Cell sorting was performed using FACSAria (BD Biosciences), and flow cytometry data were collected on FACSCanto (BD Biosciences). Fluorescence-activated cell sorting (FACS) data were analyzed using FlowJo software versions 9 and 10 (TreeStar).

RNA-seq Analysis. RNA-sequencing data of WT and *Tet2* KO naïve, Th1, and Tfh SMARTA CD4+ T cells were accessed from GSE183316. Analysis of differentially expressed genes was carried out as described in ref. 13. Briefly, mapped reads were assigned to annotated genes using featureCounts version 1.6.3, and differentially expressed genes were identified using DESeq2 version 1.30.1 with a 5% false discovery rate (33).

DNA Library Preparation and Whole-Genome Enzymatic Methyl Sequencing. Genomic DNA was isolated from sorted cells using a Quick-DNA Microprep Kit (Zymo) and sonicated to generate fragments of approximately 350 to 400 base pairs using S220 Focused Ultrasonicator (Covaris). Unmethylated cytosines were converted to uracils, and sequencing libraries were created using the NEBnext Enzymatic Methyl Seq Kit (New England Biolabs) according to the manufacturer's instructions. DNA libraries were sequenced using an Illumina NovaSeq 6000 system following the manufacturer's protocols.

Genome-Wide Methylation Analysis. Genome-wide methylation analysis for secondary WT and *Tet2* KO Th1 and Tfh SMARTA cells was carried out as follows:

Sequencing data quality was assessed using FastQC v0.11.4. Adapters were trimmed from the sequencing reads using Trim Galore! v0.4.4 using options (trim_galore -o $OUTDIR --fastqc --paired $FORWARD_READS $REVERSE_READS). Alignment to the mm10 reference genome was performed using Bismark (34) v0.19.0 with options (bismark --multicore 6 --bowtie2 -N 1 $MM10 -1 $FORWARD_READS -2 $REVERSE_READS). Deduplication was performed with deduplicate_bismark (34) (deduplicate_bismark -p -bam $BISMARK_ALIGNED_BAM). Library quality was assessed on the basis of the percentage of reads that aligned to the genome. Library quality was considered sufficient if greater than 50% of reads uniquely aligned to the genome. Enzymatic methyl conversion efficiency was assessed by evaluating the percent of methylation observed in the CHH genome (where H is any base except G) context. Enzymatic methyl conversion was considered sufficient when this value was less than 3%. Genome coverage was assessed using the bedtools (35) genomecov software v2.25.0. Library genome coverage was considered sufficient if 80% of the genome had a depth of at least 10 reads. For each library that met these quality metrics, methylation percentages at individual CpG positions in the reference genome were quantified using the Bismark Methylation Extractor (34) v0.19.0 program with options (bismark_methylation_extractor-p--comprehensive--bedgraph $BISMARK_DEDUPLICATED_BAM). DMRs among the datasets were detected using BSmooth DMR finder (36). DMRs have at least 10 CpGs and an absolute mean difference of >0.1. DMRs were then ranked by mean difference between secondary Tfh and secondary Th1. Visualization of CpG positions with at least 10× coverage on colored heatmaps (blue-white-red) reflects the percent methylated from 0 to 100%. Individual genomic loci were displayed using UCSC Genome Browser (37). Genome-wide methylation data of primary WT and *Tet2* KO naïve, Th1, and Tfh SMARTA CD4+ T cells were accessed from GSE182940. Analysis of DMRs was carried out as described in ref. 13.

Data, Materials, and Software Availability. Whole genome enzymatic methylation sequencing data of sorted secondary effector CD4+ T cell subsets are available on the Gene Expression Omnibus database under the accession number GSE239724 (38). Previously published data were used for this work, including RNA-sequencing data used that are found at the Gene Expression Omnibus database under the accession number GSE183316 (39), and whole genome enzymatic methylation sequencing data of naive and day 7 effector CD4+ T cells subsets, that are available on the Gene Expression Omnibus database under accession number GSE182940 (40). All other data are included in the manuscript and/or *SI Appendix*.

1. R. V. Luckheeram, R. Zhou, A. D. Verma, B. Xia, CD4+T cells: Differentiation and functions. *Clin. Dev. Immunol.* **2012**, 925135 (2012).
2. J. A. Juno *et al.*, Cytotoxic CD4 T cells-friend or foe during viral infection? *Front. Immunol.* **8**, 19 (2017).
3. I. Yusuf *et al.*, Germinal center T follicular helper cell IL-4 production is dependent on signaling lymphocytic activation molecule receptor (CD150). *J. Immunol.* **185**, 190–202 (2010).
4. C. G. Vinuesa, M. A. Linterman, D. Yu, I. C. MacLennan, Follicular helper T cells. *Annu. Rev. Immunol.* **34**, 335–368 (2016).
5. H. Qi, T follicular helper cells in space-time. *Nat. Rev. Immunol.* **16**, 612–625 (2016).
6. S. Crotty, T follicular helper cell biology: A decade of discovery and diseases. *Immunity* **50**, 1132–1148 (2019).
7. D. J. Gasper, M. M. Tejera, M. Suresh, CD4 T-cell memory generation and maintenance. *Crit. Rev. Immunol.* **34**, 121–146 (2014).
8. C. J. Lio, A. Rao, TET enzymes and 5hmC in adaptive and innate immune systems. *Front. Immunol.* **10**, 210 (2019).
9. J. S. Hale *et al.*, Distinct memory CD4+ T cells with commitment to T follicular helper- and T helper 1-cell lineages are generated after acute viral infection. *Immunity* **38**, 805–817 (2013).
10. K. Ichiyama *et al.*, The methylcytosine dioxygenase Tet2 promotes DNA demethylation and activation of cytokine gene expression in T cells. *Immunity* **42**, 613–626 (2015).
11. X. Yue *et al.*, Control of Foxp3 stability through modulation of TET activity. *J. Exp. Med.* **213**, 377–397 (2016).
12. X. Yue *et al.*, Whole-genome analysis of TET dioxygenase function in regulatory T cells. *EMBO Rep.* **22**, e52716 (2021).
13. A. Baessler *et al.*, Tet2 coordinates with Foxo1 and Runx1 to balance T follicular helper cell and T helper 1 cell differentiation. *Sci. Adv.* **8**, eabm4982 (2022).
14. R. S. Akondy *et al.*, Origin and differentiation of human memory CD8 T cells after vaccination. *Nature* **552**, 362–367 (2017).
15. S. A. Carty *et al.*, The loss of TET2 promotes CD8(+) T cell memory differentiation. *J. Immunol.* **200**, 82–91 (2018).
16. A. Oxenius, M. F. Bachmann, R. M. Zinkernagel, H. Hengartner, Virus-specific MHC-class II-restricted TCR-transgenic mice: effects on humoral and cellular immune responses after viral infection. *Eur. J. Immunol.* **28**, 390–400 (1998).
17. J. Choi *et al.*, Bcl-6 is the nexus transcription factor of T follicular helper cells via repressor-of-repressor circuits. *Nat. Immunol.* **21**, 777–789 (2020).
18. Y. Huang *et al.*, Distinct roles of the methylcytosine oxidases Tet1 and Tet2 in mouse embryonic stem cells. *Proc. Natl. Acad. Sci. U.S.A.* **111**, 1361–1366 (2014).
19. K. D. Rasmussen *et al.*, TET2 binding to enhancers facilitates transcription factor recruitment in hematopoietic cells. *Genome Res.* **29**, 564–575 (2019).
20. X. Liu *et al.*, Transcription factor achaete-scute homologue 2 initiates follicular T-helper-cell development. *Nature* **507**, 513–518 (2014).
21. K. Hollister *et al.*, Insights into the role of Bcl6 in follicular Th cells using a new conditional mutant mouse model. *J. Immunol.* **191**, 3705–3711 (2013).
22. L. A. Shaw *et al.*, Id2 reinforces TH1 differentiation and inhibits E2A to repress TFH differentiation. *Nat. Immunol.* **17**, 834–843 (2016).
23. R. L. Rutishauser *et al.*, Transcriptional repressor Blimp-1 promotes CD8(+) T cell terminal differentiation and represses the acquisition of central memory T cell properties. *Immunity* **31**, 296–308 (2009).
24. Y. S. Choi *et al.*, Bcl6 expressing follicular helper CD4 T cells are fate committed early and have the capacity to form memory. *J. Immunol.* **190**, 4014–4026 (2013).
25. T. Ciucci *et al.*, Dependence on Bcl6 and Blimp1 drive distinct differentiation of murine memory and follicular helper CD4+ T cells. *J. Exp. Med.* **219**, e20202343 (2021).

26. C. Havenar-Daughton *et al.*, Direct probing of germinal center responses reveals immunological features and bottlenecks for neutralizing antibody responses to HIV Env trimer. *Cell Rep.* **17**, 2195–2209 (2016).

27. K. M. Cirelli *et al.*, Slow delivery immunization enhances hiv neutralizing antibody and germinal center responses via modulation of immunodominance. *Cell* **177**, 1153–1171.e1128 (2019).

28. J. H. Lee *et al.*, Modulating the quantity of HIV Env-specific CD4 T cell help promotes rare B cell responses in germinal centers. *J. Exp. Med.* **218**, e20201254 (2021).

29. D. R. Burton *et al.*, A blueprint for HIV vaccine discovery. *Cell Host Microbe* **12**, 396–407 (2012).

30. M. A. Linterman, D. L. Hill, Can follicular helper T cells be targeted to improve vaccine efficacy? *F1000Res* **5**, 1–12 (2016), 10.12688/f1000research.7388.1.

31. M. Ko *et al.*, Ten-Eleven-Translocation 2 (TET2) negatively regulates homeostasis and differentiation of hematopoietic stem cells in mice. *Proc. Natl. Acad. Sci. U.S.A.* **108**, 14566–14571 (2011).

32. R. J. Johnston *et al.*, Bcl6 and Blimp-1 are reciprocal and antagonistic regulators of T follicular helper cell differentiation. *Science* **325**, 1006–1010 (2009).

33. M. I. Love, W. Huber, S. Anders, Moderated estimation of fold change and dispersion for RNA-seq data with DESeq2. *Genome Biol.* **15**, 550 (2014).

34. F. Krueger, S. R. Andrews, Bismark: A flexible aligner and methylation caller for Bisulfite-Seq applications. *Bioinformatics* **27**, 1571–1572 (2011).

35. A. R. Quinlan, I. M. Hall, BEDTools: A flexible suite of utilities for comparing genomic features. *Bioinformatics* **26**, 841–842 (2010).

36. K. D. Hansen, B. Langmead, R. A. Irizarry, BSmooth: From whole genome bisulfite sequencing reads to differentially methylated regions. *Genome Biol.* **13**, R83 (2012).

37. W. J. Kent *et al.*, The human genome browser at UCSC. *Genome Res.* **12**, 996–1006 (2002).

38. A. Baessler *et al.*, Tet2 deletion in CD4+ T cells disrupts Th1 lineage commitment in memory cells and enhances T follicular helper cell recall responses. Gene Expression Omnibus. https://www.ncbi.nlm.nih.gov/geo/query/acc.cgi?acc=GSE239724. Deposited 31 July 2023.

39. A. Baessler, J. S. Hale, Tet2-mediated epigenetic programing of T follicular helper cell differentiation (RNA-Seq). Gene Expression Omnibus. https://www.ncbi.nlm.nih.gov/geo/query/acc.cgi?acc=GSE183316. Deposited 2 September 2021.

40. A. Baessler, J. S. Hale, Tet2-mediated epigenetic programing of T follicular helper cell differentiation (Methyl-Seq). Gene Expression Omnibus. https://www.ncbi.nlm.nih.gov/geo/query/acc.cgi?acc=GSE182940. Deposited 27 August 2021.